

Surface Stress Effects in Indentation Fracture

DAVID J. GREEN and RAJAN TANDON

Department of Materials Science & Engineering, The Pennsylvania State University, University Park, PA 16802, USA

ABSTRACT

It has been suggested previously that indentation crack size can be used to determine the state of residual surface stress in a brittle material. The aim of this paper is to review and extend the fracture mechanics associated with the formation of indentation cracks on such surfaces. The analysis is compared to experimental data for a soda lime silica glass containing a thin layer of surface residual compression. It is shown that the value of the surface stress obtained based by the analysis is in disagreement with the values obtained by independent techniques. Further analysis of the data concludes that the indentation approach significantly underestimates the surface stress. It is proposed that the discrepancy is the result of the equilibrium crack shape being substantially different from the assumed semi-circular shape and experimental evidence is given to support this hypothesis.

KEYWORDS

Surface stress, indentation cracks, surface cracks, crack shape, brittle fracture

INTRODUCTION

It has been suggested that the measurement of indentation crack size in brittle materials can be used to measure the state of residual surface stress (Marshall and Lawn, 1987, Lawn and Fuller, 1984, Gruninger *et al*, 1987). This approach depends on understanding the fracture mechanics involved in crack formation on such surfaces. Moreover, as the introduction of compressive surface stresses has been established as a strengthening mechanism for brittle materials (Kirchner, 1979), it is important to understand the effect of contact damage on such surfaces and their subsequent reliability. The introduction of controlled indentation cracks represents a scientific approach towards the study of these effects. The aim of this paper is to measure the indentation crack sizes for glasses that contain a thin ion-exchanged surface layer. The approach in the paper will be to discuss the fracture mechanics solutions for residually-stressed surfaces and to compare the analysis with the experimental data.

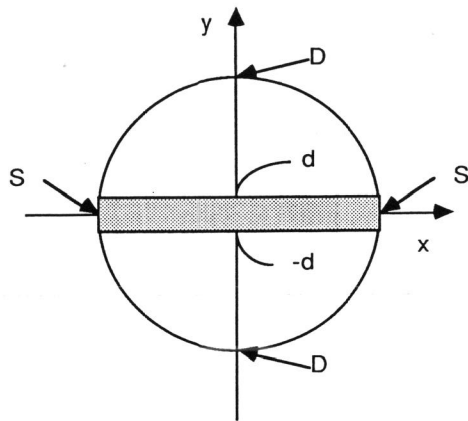


Fig. 1. Circular crack subjected to a stress over a strip-like area (after the approach of Lawn and Fuller, 1984).

THEORETICAL BACKGROUND

A stress intensity factor solution for a circular crack, radius c , subjected to stresses over mirror-symmetric strips has been developed previously (Lawn and Fuller 1984). For this paper, let us consider the special case in which the strips form a single symmetric band with respect to one of the cartesian axes. The geometry is shown in Fig. 1 and was solved by considering the influence of a point force on the stress intensity factor for the points marked S (Lawn and Fuller 1984). The point force solution was already available (Tada *et al*, 1973) and thus the final solution involved integration over the stressed area. The stress intensity factor (K_S) at the points marked S was determined to be

$$K_S = \left(\frac{\psi}{c^{1/2}} \right) \int_0^d \left[\left(\frac{c}{y} \right)^{1/2} - 1 \right] \sigma_R(y) dy \quad (1)$$

where $\sigma_R(y)$ is the stress acting over the strip and ψ is the crack geometry term ($2/\sqrt{\pi}$). For the surface stress problem, the same solution is considered to apply with the surface crack being considered semi-circular. For the surface crack case, ψ will include a surface correction term. If $\sigma_R(y)$ is known, a simple integration can be performed to obtain K_S . For example, if $\sigma_R(y)$ is uniform, one obtains for $d \leq c$

$$K_S = \psi \sigma_R d^{1/2} \left[2 - \left(\frac{d}{c} \right)^{1/2} \right] \quad (2)$$

For $d \geq c$, the upper integration limit in Eqs. 1 and 2 is replaced by c and Eq. 2 reduces to the well-known solution $K_S = \psi \sigma_R \sqrt{c}$ for a circular crack subjected to a uniform stress. In the experimental portion of this study, the residual stress profile was found to be approximately linear to a depth d and for this case, Eq. 2 becomes

$$K_S = \psi \sigma_R d^{1/2} \left[\left(\frac{4}{3} \right) - \frac{1}{2} \left(\frac{d}{c} \right)^{1/2} \right] \quad (3)$$

where σ_R is the stress at $y = 0$. In order to use Eqs. 2 and 3 for the indentation crack problem, it is necessary to assume that fracture is being controlled by K_S . This is an important assumption as there will be a variation in the stress intensity factor around the crack circumference. For example, one can use the above approach to determine the stress intensity factor (K_D) at the points marked D in Fig. 1. Using the point force solution (Tada *et al*, 1973), one obtains

$$K_D = \int_{-d}^d \int_{-(c^2-y^2)^{1/2}}^{(c^2-y^2)^{1/2}} \frac{\sigma_R(y)}{\pi(\pi c)^{1/2}} \left\{ \frac{(c^2-x^2-y^2)^{1/2}}{[(c^2-y^2)+x^2]^{1/2}} \right\} dx dy \quad (4)$$

Using the substitutions $a^2 = c^2 - y^2$ and $b^2 = (c - y)^2$, Eq. 4 can be integrated using standard tables and one obtains

$$K_D = \int_{-d}^d \frac{\sigma_R(y)}{(\pi c)^{1/2}} \left\{ \frac{(2c)^{1/2}}{(c-y)^{1/2}} - 1 \right\} dy \quad (5)$$

For the case of uniform stress, Eq. 5 can be solved to give

$$K_D = \sigma_R \psi c^{1/2} \left[\left(2 + \left[\frac{2d}{c} \right] \right)^{1/2} - \left(2 - \left[\frac{2d}{c} \right] \right)^{1/2} - \left(\frac{d}{c} \right) \right] \quad (6)$$

Figure 2 compares Eqs. 2 and 6 to show the difference between the stress intensity factor at the surface of a semi-circular crack compared to that at its deepest point. For illustrative purposes, it was assumed that ψ is the same at both points. As shown in Fig. 2, when $c \leq d$, there is no difference between K_S and K_D but once $c > d$, the difference can be substantial. For the thin-layer case ($c \gg d$), K_S approaches a limiting value $2\psi \sigma_R \sqrt{d}$ while K_D approaches zero. For a linear gradient, the limiting form of K_S for $c \gg d$ is determined from Eq. 3 as $4\psi \sigma_R \sqrt{d}/3$. In order to use these stress intensity factor solutions for the indentation crack problem, it is generally assumed that the crack remains semi-circular and that it is K_S that is controlling the indentation crack size as measured by the surface trace. The stress intensity factor solutions discussed above will also be important in determining the strength of brittle materials that contain residual surface stresses but this is the subject of a separate study (Tandon, 1988).

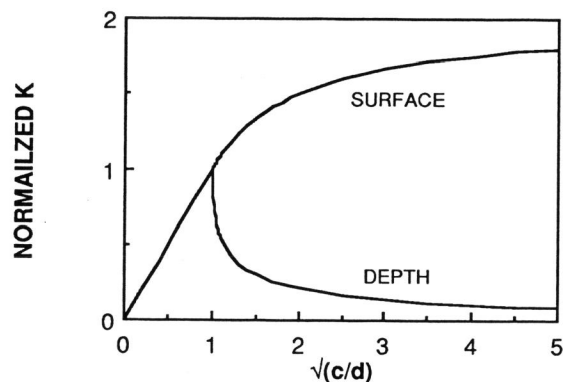


Fig. 2 Normalized stress intensity ($K/[\sigma_R \psi \sqrt{d}]$) for a circular crack subjected to a uniform stress over a strip width $2d$. The stress intensity factor is calculated for points S (surface) and D (depth) in Fig. 1.

Let us now consider the indentation crack problem for residually-stressed surfaces in more detail, especially the prediction of indent crack size. The stress intensity factor for an indentation crack will consist of two terms. The first term is that due to the residual stress associated with the inelastic indentation zone and the second is that due to the residual surface stress. The first term has been established elsewhere (Anstis *et al*, 1981) and for the second term we will use Eq. 2, as discussed above (uniform stress to a depth d). The total stress intensity factor for the indentation crack is given by

$$K = \frac{\chi P}{c^{3/2}} + \psi \sigma_R d^{1/2} \left[2 - \left(\frac{d}{c} \right)^{1/2} \right] \quad (7)$$

where χ is an elastic-plastic indentation term (Anstis *et al*, 1981) and P is the indentation load. For cases in which $d < c$, it has been shown that stresses below the surface can play a role (Gruninger *et al*, 1987) but we will assume they can be neglected. Such stresses were measured for coated glass but their magnitude was typically < 1 MPa and much less than the compressive stresses in the thin coatings (-34 to -87 MPa) (Gruninger *et al*, 1987). In order to use Eq. 7 to predict indentation crack size, two approaches have been used. In the first case, the indentation crack sizes are measured immediately after indentation, for which $K = K_{IC}$, the fracture toughness of the material (Lawn and Marshall, 1977, Lawn and Fuller, 1984). The other approach recognizes that sub-critical crack growth occurs in many ceramic materials, allowing the indentation crack to increase further in length. The crack does reach an equilibrium length as K approaches the threshold stress intensity factor (K_{IT}). Thus, one could relate the equilibrium crack size to the surface stress. We will denote both conditions by K_C^* as the final equations are the same but the value of K_C^* (K_{IC} or K_{IT}) will depend on the experimental procedure that is utilized. Both experimental approaches generally assume that K_C^* is not influenced by the

modified surface. We will compare the predicted indentation crack size with that expected on a stress-free surface. Denoting the crack sizes on the residually-stressed and stress-free surfaces by c_R and c_0 , we can use Eq. 7 with $K = K_C^* = \chi P / c_0^{3/2}$ to obtain for $d \leq c$.

$$\frac{P}{c_R^{3/2}} = \frac{P}{c_0^{3/2}} \left[1 - \left(\frac{\psi \sigma_R d^{1/2}}{K_C^*} \right) \left[2 - \left(\frac{d}{c_R} \right)^{1/2} \right] \right] \quad (8)$$

For $d \geq c$, one obtains

$$\frac{P}{c_R^{3/2}} = \frac{P}{c_0^{3/2}} \left[1 - \frac{\psi \sigma_R c_R^{1/2}}{K_C^*} \right] \quad (9)$$

Equations 8 and 9 can be used in a variety of ways but of interest here is the measurement of surface residual stress by comparing indentation crack lengths on stress-free and residually-stressed surfaces. The value of σ_R can be estimated from such data, provided ψ , d and K_C^* are known. Equations 8 and 9 have been used in previous studies to measure σ_R from indentation crack lengths (Marshall and Lawn, 1987, Lawn and Fuller, 1984, Gruninger *et al*, 1987). In the applications of Eq. 8, the cases of interest (Lawn and Fuller, 1984, Gruninger *et al*, 1987) were those in which $d < c$. For this situation, Eq. 8 becomes

$$\frac{P}{c_R^{3/2}} = \frac{P}{c_0^{3/2}} - \frac{2\psi \sigma_R d^{1/2}}{\chi} \quad (10)$$

Thus provided the values of ψ , χ (or K_C^*) and d are known, the value of σ_R can be estimated. This approach was used to measure the surface residual stress on irradiated glass (Lawn and Fuller, 1984) and coated glass (Gruninger *et al*, 1987). For the current study in which the residual stress profile is approximately linear, Eq. 10 becomes

$$\frac{P}{c_R^{3/2}} = \frac{P}{c_0^{3/2}} - \frac{4\psi \sigma_R d^{1/2}}{3\chi} \quad (11)$$

Eq. 9 has been used to measure the residual stress in a thermally-tempered glass plate (assuming uniform stress and $d > c$), by plotting the normalized crack size parameter against the \sqrt{c} and obtaining σ_R from the slope (Marshall and Lawn, 1977). The purpose of the present study was to utilize Eq. 11 for a glass into which a thin layer of surface compression was introduced by ion exchange.

EXPERIMENTAL PROCEDURE

Commercial soda-lime-silica glass was obtained in the form of plates and was machined into 30 x 4 x 2.2 mm bars. Prior to the indentation experiments, the bars were annealed at a temperature of 520° C for 24 hours. Indentations were placed on the bars prior to annealing and the stress birefringence pattern around the indentation was observed. The disappearance of the stress birefringence was taken as an indication that the annealing cycle was effective.

The annealed samples were cleaned and ion-exchanged. Ion-exchange was accomplished by placing the samples in a constant temperature bath of molten KNO₃. The temperature of the bath was maintained at 414° C, well below the annealing point. The Na⁺ ions in the glass are exchanged for the K⁺ ions in the salt according to the reaction Na⁺ ↔ K⁺. The exchange by the larger K⁺ ions is the source of surface compression. After the requisite period of exchange (30 minutes and 4 hours), the samples were removed from the bath, washed in water to remove the adhering salt and dried.

These exchanged samples were then indented in air using a Vicker's diamond indenter. The load range used was 20-80 N. The lower limit was dictated by the difficulty in nucleating the cracks below that load and the upper limit by the occurrence of lateral crack chipping and spalling. The crack lengths on these samples were measured immediately after indentation. More than 50 measurements of the crack length were made at each load for the two conditions of exchange. Similar measurements were made on samples with stress-free surfaces.

A strain gage technique was utilized to estimate the surface compression. The technique has been discussed by Virkar et al [9] and consists of placing a strain gage on one surface of the exchanged sample and polishing away the other surface. The force imbalance due to the surface removal causes a bending moment in the sample. The tensile strain values read by the gage is due to this moment and changes in the overall force balance and can be related to the prior compressive surface stress (Virkar et al, 1988). For thin residually-stressed surface layers, this analysis can be used to show there is a dramatic change in the slope of strain-removal depth slope once the compressive layer is removed (Tandon, 1988). Essentially one obtains a plateau in the strain values for small removal depths once the compressive layer is removed. The plateau strain values can be used to calculate the surface residual stress using the prior analysis (Virkar et al, 1988). For this study, the residual stress was assumed to have a linear gradient and an equation was derived to relate the plateau strain to the surface residual stress. For this case, the plateau strain (ϵ_p) can be related to the strain differential ($\Delta\epsilon_o$) between the layers of residual tension and compression according to the relation

$$\Delta\epsilon_o = \frac{D_2\epsilon_p}{2D_1} \quad (12)$$

where D_1 and D_2 are the depths of the regions under compression and tension respectively (Tandon, 1988). For thin layers, Eq. 12 can be used to determine the stress in the compression layer prior to bending using

$$\sigma = \frac{E\Delta\epsilon_o}{(1-\nu)} \quad (13)$$

where E and ν are the Young's modulus and Poisson's ratio of the exchanged layer. For these calculations it was assumed the elastic constants were the same as the unexchanged glass.

The concentration profile of the K⁺ diffusion was determined using a Kevex analyzer attached to an SEM. This profile serves as a good measure of the depth of penetration of the K⁺ ion and can also be used to calculate the surface stress value by assuming the residual surface stress is simply a result of the difference between the ionic sizes of Na and K. The residual stress was calculated from Eq. 13 with ($\Delta\epsilon_o$) = $F(\Delta V/V)/3$, where F is the fraction of ions exchanged and ($\Delta V/V$) is the fractional volume change due to the incorporation of the larger potassium ions.

To delineate the crack shape, some exchanged samples with indent cracks were placed in a salt bath containing AgNO₃ at 265°C for 3 days. It was expected that the Ag would penetrate into the crack and exchange with Na ions on the crack surface. These samples were then fractured and examined in the backscattering mode of the SEM. The atomic number contrast could then be used to delineate the indentation crack shape.

RESULTS AND DISCUSSION

The potassium ion composition profiles obtained for the two exchange conditions are shown in Fig. 3. The profiles could be approximated to a linear gradient and the

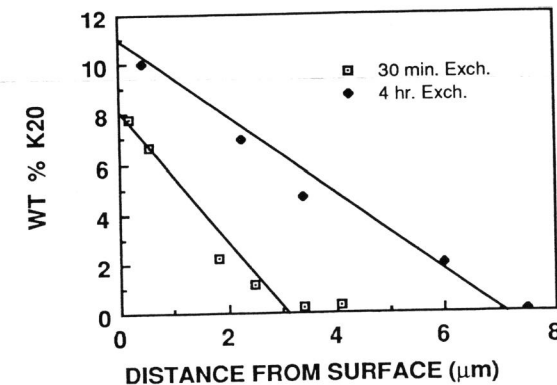


Fig. 3. Potassium ion composition profiles for specimens exchanged for 30 and 240 minutes as a function of distance from the external surface.

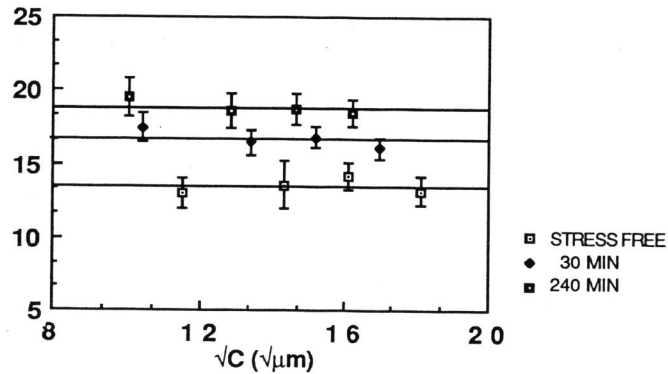


Fig. 4. The indentation crack size parameter $P/c^{3/2}$ for a soda lime silica glass ion-exchanged for two different times (30 and 240 minutes) and the values obtained on a stress-free surface.

depths of exchange were estimated to be 3 and 7.5 μm respectively for the 30 min and 240 min. exchange times. The results of the indentation cracks size measurements are shown in Fig. 4 in terms of $P/c^{3/2}$ as a function of \sqrt{c} , where $c = c_D$ or c_R . Values of d/c were in the range 0.01 to 0.08, allowing the thin layer solution of Eq. 11 to be utilized to calculate σ_R . This was accomplished by fitting a horizontal line to the data to determine the average value of $P/c^{3/2}$ for the three conditions. The difference in $P/c^{3/2}$ between for the residually-stressed and stress-free values allows the calculation of $-4\psi\sigma_R\sqrt{d}/3\chi$ (Eq. 11). Functions for the estimation ψ and χ are available in the literature but for the sake of accuracy, values that were available for this particular glass in its annealed condition were used (Tandon, 1988). The parameter χ was determined from a fracture toughness value of 0.73 $\text{MPa}\cdot\sqrt{\text{m}}$, that was obtained using the single edge-notched beam technique (three point bending) (Tandon, 1988). From the analysis of indentation crack length measurements (immediately after indentation) on a stress-free glass surface, $\chi = K_{IC}c_0^{3/2}/P$ (Anstis et al, 1981). A value of $\chi = 0.54$ was obtained using this analysis. The value of ψ was obtained by measuring the crack size (surface trace) of annealed indentation cracks and subsequently measuring the fracture strength of the indented materials. Using standard fracture mechanics, $\psi = K_{IC}/[\sigma_f\sqrt{c}]$, where σ_f is the fracture strength, a value of $\psi = 0.73$ was obtained.

The values of σ_R calculated from the experimental crack length data for the two exchange conditions, using Eq. 11 and the above values of ψ , χ and d , are given in Table 1. The results are compared with the residual surface stress value obtained from the surface removal technique (Tandon, 1988). As can be seen, the indentation crack length measurements appear to severely underestimate the surface stress. In order to confirm the residual stress values obtained from the surface removal technique are reasonable, residual stresses were estimated based on the difference

Table 1. Calculated values of surface residual stress (MPa) from different techniques

TECHNIQUE	EXCHANGE TIME (min)	
	30	240
INDENT CRACK SIZE	-105	-110
SURFACE REMOVAL	-800	-920
COMPOSITION	-620	-850

between the size of sodium and potassium ions (Tandon, 1988). Using the data given in Fig. 3, values of σ_R for the two conditions (30 and 240 min. exchange times) were estimated to be -620 and -850 MPa respectively (Table 1). In addition, the strengthening associated with the fracture of non-indented specimens has been found to be 300 to 400 MPa (Tandon, 1988). If one assumes the surface compression is the cause of this strengthening, the surface stress must equal or exceed the negative value of the strengthening. There appears to be no doubt therefore that the surface removal values of σ_R are reasonable and the indentation crack lengths cannot be used to determine the surface stress with the analysis outlined in Section 1. Similar problems have been encountered in attempting to determine the surface stress from indentation strength measurements on the same glass (Tandon, 1988). Indeed, it was also found that flaw history, i.e., whether the glass is exchanged before or after indentation can significantly influence the strength measurements (Tandon, 1988).

The critical question that remains from this study is the cause of the discrepancy. As pointed out in Section 1, the stress intensity factor due to the surface compression can vary substantially around the periphery of a semi-circular crack. For the thin layer case studied here, ignoring the stress intensity factor due to the indentation, $K_D \sim 0$, whereas K_S calculated from $4\psi\sigma_R\sqrt{d}/3$ using the values of σ_R obtained from the surface removal measurements, gives a value in the range -1.3 to -2.4 $\text{MPa}\cdot\sqrt{\text{m}}$. Thus, there would be a large difference in the predicted crack size if one were to use K_D instead of K_S in the fracture analysis. The experimental results indicate that the final crack length is intermediate between these extremes, implying there must be a compromise between K_D and K_S in determining the final crack size. For these experiments in which the indentation crack length is measured immediately after indentation, one would expect that $K = K_{IC}$ for all points around the crack periphery. Thus, the assumption of a semi-circular crack must be at odds with the actual crack shape. In response to these effects, the crack would be expected to find an equilibrium shape after indentation that is not semi-circular. Figure 5 shows a schematic illustration of the effect. The outer semi-circular crack is that predicted using K_D while the inner would be based on the value of K_S . For the thin layer case, the surface stresses are not expected to change the crack depth as the median crack usually forms below the surface in response to the indentation load. During unloading, however, as the crack propagates back to the surface, a compromise must be made

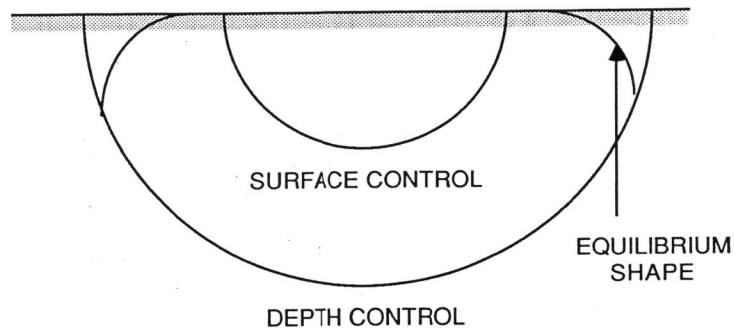


Fig. 5. Schematic illustration of the change in crack shape that results from a thin layer of surface stress. The final crack shape is a compromise between that predicted from the stress intensity factors at the surface and deepest points of a semi-circular crack (surface compression case)

and the surface trace is longer than predicted from K_{IS} . Although a theoretical treatment is not yet available, experimental evidence was found for an equilibrium crack shape that is clearly not semi-circular. This was accomplished by indenting an ion-exchanged sample and subjecting it to a further ion-exchange using $AgNO_3$ instead of KNO_3 . The purpose of the second exchange was to allow the indent crack surfaces to be exchanged, allowing a definition of the crack shape. The specimen was subsequently fractured and viewed using the back-scattered mode in the scanning electron microscope. The atomic number contrast from the Ag ions allows the crack shape to be highlighted. Figure 6 shows the results of this experiment and although only a segment of the indentation crack was observed clearly, it was found that the crack front does not form a circular segment and the crack radius slightly below the surface is substantially larger than the surface trace. It is concluded that the equilibrium crack shape is not semi-circular for the indentation of glasses containing a thin ion-exchanged layer and that further theoretical and experimental studies are needed to understand the factors controlling indentation crack size on such surfaces.

CONCLUSIONS

Previous studies have suggested that indentation crack size can be used to determine the state of residual surface stress in a brittle material. The theoretical analysis indicated that semi-circular surface cracks would have a variation in stress intensity factor around the crack periphery. Assuming the surface trace of the radial cracks is controlled by the stress intensity factor at the surface of a semi-circular crack, one can predict the surface stress from indentation crack length measurements. This analysis was compared to experimental data for a soda lime silica glass containing a thin layer of surface residual compression. It was shown that the value of the surface stress obtained based on the analysis is in disagreement with the values obtained by an independent technique. Further analysis of the data

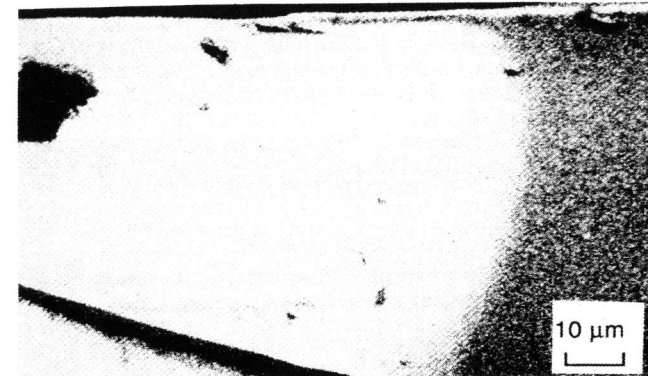


Fig. 6. Micrograph showing the change in crack shape that occurs in the vicinity of the external surface for a glass containing a thin layer of surface compression. The indentation crack surface was ion-exchanged using silver ions to give atomic number contrast (back-scattered mode, scanning electron microscope)

concludes that the indentation approach significantly underestimates the surface stress. It is proposed that the discrepancy is the result of the equilibrium crack shape being substantially different from the assumed semi-circular shape and experimental evidence is given to support this hypothesis. This effect is a result of the compromise that is needed between the stress intensity factors at the surface and deepest point of the crack. For thin layers, this compromise leads to increase in the length of the surface crack trace compared to the predicted value.

ACKNOWLEDGEMENTS

The authors wish to acknowledge the technical assistance and discussions with other members of the Department of Materials Science and Engineering. The work was financially supported by the U. S. Department of Energy under Grant No. DE-FG02-86ER45252.

REFERENCES

- Anstis, G. R., P. Chantikul, B. R. Lawn and D. B. Marshall, (1981). A critical evaluation of indentation techniques for measuring fracture toughness: I, Direct crack measurements. *J. Am. Ceram. Soc.*, **64**, 533-38.
- Gruninger, M. F., B. R. Lawn, E. N. Farabaugh and J. B. Wachtman, Jr., (1987). Measurement of residual stresses in coatings on brittle substrates by indentation fracture. *J. Am. Ceram. Soc.*, **70**, 344-48.
- Kirchner, H. P., (1979). *Strengthening of Ceramics*. Marcel Dekker, Inc., New York.
- Lawn, B. R. and E. R. Fuller Jr., (1984). Measurement of thin-layer surface stresses by indentation fracture. *J. Mater. Sci.*, **19**, 4061-65.

- Marshall, D. B. and B. R. Lawn, (1977). An indentation technique for measuring stresses in tempered glass surfaces. *J. Am. Ceram. Soc.*, 60 [1-2] 86-87.
- Tada, H., P. C. Paris and G. R. Irwin (1973). *The Stress Analysis of Cracks Handbook*. Del Research Corporation, Hellertown, PA, p 24.2.
- Tandon, R. (1988). *Indentation Behavior of Ion-Exchanged Glass*. M. S. Thesis, The Pennsylvania State University.
- Virkar, A. V., J. F. Jue, J. J. Hansen and R. A. Cutler, (1988). Measurement of residual stresses in oxide-ZrO₂ three-layer composites. *J. Am. Ceram. Soc.*, 71, C-148-51.